主論文　リポジトリ掲載分

Macular Choroidal Thickness and Volume of Eyes with Reticular Pseudodrusen Using Swept-Source Optical Coherence Tomography

NAOKO UEDA-ARAKAWA, SOTARO OOTO, ABDALLAH A. ELLABBAN, AYAKO TAKAHASHI, AKIO OISHI, HIROSHI TAMURA, KENJI YAMASHIRO, AKITAKA TSUJIKAWA, NAGAHISA YOSHIMURA

Department of Ophthalmology and Visual Sciences, Kyoto University Graduate School of Medicine, Kyoto, Japan

Short title**:** Macular choroidal thickness in reticular pseudodrusen

Supplementary Materials (Supplementary Tables 1-3) available at AJO.com.

Inquiries to Sotaro Ooto, Assistant Professor, Department of Ophthalmology and Visual Sciences, Kyoto University Graduate School of Medicine, 54 Kawahara-cho, Shogoin, Sakyo-ku, Kyoto 606-8507, Japan
Telephone: +81-75-751-3248; Fax: +81-75-752-0933
E-mail: ohoto@kuhp.kyoto-u.ac.jp

American Journal of Ophthalmology 2014;157:994-1004.
Accepted for publication Jan 21, 2014.

Abstract

PURPOSE: To investigate the choroidal thickness/volume of eyes with reticular pseudodrusen using high-penetration swept-source optical coherence tomography (SS-OCT) and to evaluate the choroidal vasculature changes using en face images.

DESIGN: Prospective cross sectional study.

METHODS: Thirty-eight eyes with reticular pseudodrusen and 14 normal eyes were studied with prototype SS-OCT. Eyes with reticular pseudodrusen were classified into 3 subgroups: eyes without late age-related macular degeneration (AMD) (Group1), eyes with neovascular AMD (Group2), and eyes with geographic atrophy (Group3). Mean regional choroidal thickness/volume measurements were obtained by three-dimensional (3D) raster scanning. The choroidal vascular area was measured using en face images reconstructed from a 3D SS-OCT data set.

RESULTS: Mean age and axial length did not differ between eyes with reticular pseudodrusen and normal eyes. The mean choroidal thickness and volume of each sector was significantly reduced in eyes with reticular pseudodrusen compared with normal eyes ($P < .020$ for all). Mean choroidal thickness and volume of each area showed no significant difference between the 3 groups; however, most of them showed decreased thickness compared with normal eyes. En face images through the choroid revealed narrow and sparse choroidal vessels in eyes with reticular pseudodrusen. The area of choroidal vasculature was significantly reduced in eyes with reticular pseudodrusen compared with normal eyes ($P = .037$).

CONCLUSIONS: In eyes with reticular pseudodrusen, macular choroidal thickness/volume was reduced regardless of choroidal neovascularization/geographic atrophy. Thinned vessels in the choroid suggest choroidal involvement in the pathogenesis of reticular pseudodrusen.

Reticular pseudodrusen were first identified using blue-light fundus photography in 1990.[1] Arnold and associates[2] described reticular pseudodrusen as a yellowish interlacing network of oval-shaped or roundish lesions with a diameter of 125–250 μm that were visible by red-free fundus photography and infrared scanning-laser ophthalmoscopy (SLO). Recently, reticular pseudodrusen have been recognized as an additional distinctive morphologic feature observed in age-related macular degeneration (AMD).[3] Furthermore, existing evidence suggests that reticular pseudodrusen are associated with a high risk of progression to late AMD[4–11] and reduction in visual function.[12,13] The development of imaging methods, such as SLO and optical coherence tomography (OCT), has led to additional insight into its pathogenesis.[14–16]

Several researchers have reported impaired choroidal filling on indocyanine green angiography (IA) in eyes with reticular pseudodrusen.[14] It has been reported that the arrangement and pattern of reticular pseudodrusen may be related to the choroidal stroma and the choroidal vasculature.[2,17,18] A histologic study showed that the number of choroidal blood vessels was decreased in an eye with reticular pseudodrusen.[2] These findings suggest that the mechanism underlying the pathogenesis of reticular pseudodrusen may involve changes in the choroidal vasculature.

Imaging of the choroid with commercially available OCT does not allow visualization of the entire choroidal structure, owing to its low penetration and high backscattering at the level of the retinal pigment epithelium (RPE). However, since Spaide and associates[19] introduced enhanced depth imaging OCT (EDI-OCT), an increasing number of investigators have studied choroidal thickness in healthy and diseased eyes.[20–25] In fact, using the EDI- OCT technique, several researchers have reported that the choroidal thickness was decreased in eyes with reticular pseudodrusen compared with eyes without them.[17,26] However, EDI-OCT is usually coupled with multiple scan averaging to achieve high contrast and low speckle noise, resulting in less detailed raster scan images. For this reason, previous studies have focused on choroidal thickness at several measurement points.

Recently, other investigators measured the choroidal thickness by using OCT at a longer wavelength.[27–29] In these more recent studies, higher penetration of the OCT probe light, which uses a center wavelength of approximately 1000 nm instead of the current OCT probing light operated at approximately 800 nm, allows the visualization of the entire choroid without resorting to the EDI system or multi-averaging. Swept-source OCT (SS-OCT) at a longer wavelength is characterized by a high-speed scan rate and a relatively low sensitivity roll- off vs depth compared with the spectral-domain OCT, and it allows a 3-dimensional (3D) high-contrast image of the choroid to be captured. In this

study, we scanned the whole macular area in eyes with reticular pseudodrusen by high-penetration SS-OCT, using a 3D raster scan protocol, and produced a choroidal thickness map of the macular area. By applying the sectors described in the Early Treatment Diabetic Retinopathy Study (ETDRS) to this map, we measured the mean choroidal thickness and volume in each sector. In addition, we evaluated the changes in the choroidal vasculature using en face SS-OCT–derived images.

METHODS

All investigations adhered to the tenets of the declaration of Helsinki, and this study was approved by the institutional review board and the ethics committee of Kyoto University Graduate School of Medicine. After the nature and possible consequences of the study were explained, written informed consent was obtained from all the participating subjects.

SUBJECTS: For this prospective cross-sectional study, we recruited patients with reticular pseudodrusen who visited the Macular Service at Kyoto University Hospital, Kyoto, Japan, between July 1, 2010 and February 14, 2013, as well as age-matched normal controls. To be included in the current study, the patients had to be 50 years of age or above.

All of the patients had already been diagnosed with reticular pseudodrusen based on the appearance of reticular patterns according to at least 2 of the following imaging modalities: color fundus photography (blue channel images), infrared reflectance (IR) imaging, fundus autofluorescence (FAF), spectral-domain OCT (SD-OCT), and IA. Eyes with high myopia (axial length≧26.0 mm) and eyes with other macular abnormalities (eg, idiopathic choroidal neovascularization, angioid streaks, other secondary choroidal neovascularization, central serous chorioretinopathy, epiretinal membranes, or retinal arterial macroaneurysms); any history or signs of retinal surgery, including laser treatment and photodynamic therapy; or evidence of glaucoma or high intraocular pressure (≧22mmHg) were also excluded from this study. Subjects with systemic diseases or conditions that might affect the choroidal thickness were also excluded, such as those with diabetes mellitus or malignant hypertension. Eyes whose fellow eyes had any sign of AMD including drusen were excluded from normal controls.

Eyes with reticular pseudodrusen were classified into 3 subgroups: eyes without late AMD (neovascular AMD and geographic atrophy) (Group 1), eyes with neovascular AMD (Group 2), and eyes with geographic atrophy (Group 3). Neovascular AMD was characterized by choroidal neovascularization (CNV) detected by fluorescein angiography (FA) and IA. Geographic atrophy was detected, using color fundus

photography as a sharply delineated area (at least 175 μm in diameter) of hypopigmentation, depigmentation, or apparent absence of the RPE due to which the choroidal vessels were clearly visible.

All subjects underwent a comprehensive ocular examination, including measurement of best-corrected visual acuity (BCVA) with a 5-m Landolt chart, intraocular pressure, autorefractometry (ARK1; Nidek, Gamagori, Japan), axial length measurement using ocular biometry (IOL Master; Carl Zeiss Meditec, Jena, Germany), slit-lamp examination, color fundus photography (TRC-NW8F; Topcon Corp, Tokyo, Japan), and prototype SS-OCT. All patients with macular complications underwent simultaneous FA and IA using HRA OCT (Spectralis; Heidelberg Engineering, Heidelberg, Germany).

SWEPT-SOURCE OPTICAL COHERENCE TOMOGRAPHY SYSTEM AND SCANNING PROTOCOLS: We used an SS-OCT prototype system (Topcon, Tokyo, Japan) with an axial scan rate of 100 000 Hz operated in the 1-μm wavelength region. The details of this system were described elsewhere.[28]

SS-OCT examinations were performed by trained examiners after pupil dilation. First, horizontal and vertical line scans (12 mm) through the fovea were obtained, and ~50 B-scan images were averaged to reduce speckle noise. Second, a 3D imaging data set was acquired for each subject with a raster scan protocol of 512 (horizontal) × 128 (vertical) A-scans per data set (total: 65 536 axial scans/ volume) in 0.8 s. Each 3D scan covered an area of 6 × 6 mm centered on the fovea, which was confirmed by an internal-fixation and fundus camera integrated in the instrument. To reduce speckle noise, each image was averaged by applying the weighted moving average from 3 consecutive images. Owing to the invisible scanning light and high-speed scanning, eye movement during the 3D scan was minimal.

CHOROIDAL THICKNESS AND VOLUME MEASUREMENT PROTOCOL: The choroidal thickness was measured as the distance between the Bruch membrane (or the outer border of the RPE–Bruch membrane complex) and the chorioscleral interface (Figure 1). In each image of the 3D data set, both lines were determined manually by a trained ophthalmologist who was masked to the diagnosis, classification, or angiographic findings. Automated built-in calibration software was used to determine the distance between the 2 lines. From all 128 images of each 3D data set, a choroidal thickness map of 6 × 6 mm was created. False color was determined starting from a cool color and progressing to a warm color, at the range of 0–500 μm. After the choroidal thickness map was created, the ETDRS sectors were applied to it (Figure 1). First, the central fovea on

each image was manually registered, if necessary, to coincide with the central circle on the ETDRS segmentation diagram. The mean thickness of each sector was measured in the ‘‘center’’ sector within 0.5mm from the center of the fovea, in 4 ‘‘inner ring’’ sectors (nasal, superior, temporal, and inferior) 0.5–1.5 mm from the center of the fovea, in 4 ‘‘outer ring’’ sectors (nasal, superior, temporal, and inferior) 1.5–3 mm from the center of the fovea, and as a ‘‘whole’’ within 3 mm from the center of the fovea.

In B-scans where it was difficult to identify the whole outer choroid, 7-15 points where the chorioscleral interface could be identified were chosen and connected to create a segmentation line. After creating segmentation lines in all 128 B-scans, the choroidal thickness map was checked. If the thickness differed remarkably between adjoining B-scans, the segmentation lines of the B-scans were reexamined and corrected as required.

To examine whether the localization of reticular pseudodrusen affected the focal choroidal thickness, area of reticular pseudodrusen was assessed for Group 1 eyes using IR images. With respect to each ETDRS sector, the eyes were divided into 2 groups according to whether reticular pseudodrusen covered more than half of the area or not. The mean choroidal thickness of each ETDRS sector was compared between the 2 groups. The area of reticular pseudodrusen was assessed using the built-in software of HRA-2 (Heidelberg Engineering, Heidelberg, Germany). The data obtained were analyzed to determine the association between the areas covered by reticular pseudodrusen and mean macular choroidal thickness.

MEASUREMENT OF CHOROIDAL VASCULAR AREA USING EN FACE IMAGES: En face images were automatically reconstructed from a 3D data set using software developed by Topcon Corporation, which flattened the images at the level of Bruch membrane. Each en face image was created by averaging the consecutive images of the range of 7 μm. To analyze the area of choroidal vasculature, the en face image was adopted at the intermediate level between the Bruch membrane and the deepest site of the chorioscleral interface on the horizontal B-scan image through the fovea. To measure the area of choroidal vasculature of each adopted image, Image J software (National Institutes of Health, Bethesda, Maryland, USA) was used. In Image J, the command path of Image > Adjust > Threshold > Auto was used to differentiate the vascular area from the nonvascular area. To measure the vascular area, the command path of Analyze > Measure was used. If the adopted image contained the chorioscleral border, the image was trimmed minimally so that it contained the choroidal area only. Then, the ratio of choroidal vascular area to total area was calculated.

STATISTICAL ANALYSIS: Statistical analysis was performed using SPSS statistical software (version 20; SPSS Inc, Chicago, Illinois, USA). All values are presented as mean±standard deviation (SD). We used the unpaired *t* test or Welch's *t* test to compare the data between 2 groups with normal distribution. The Mann-Whitney *U* test was used to compare data between 2 groups in which normal distributions were not verified. To compare the data between 3 groups, 1-way analysis of variance and the Tukey-Kramer test were used. *P* values less than .05 were considered to be statistically significant.

RESULTS

In this study, 75 eyes of 44 patients with reticular pseudodrusen were examined. Among them, 12 eyes were excluded because of poor image quality (owing to unstable fixation or media opacity). Thus, the images obtained for 63 eyes from 38 patients were suitable for analysis. If both eyes were eligible for inclusion, 1 eye was selected randomly. Finally, 38 eyes from 38 patients (19 men and 19 women) with reticular pseudodrusen were included in this study. Fourteen normal eyes in 14 subjects (6 men and 8 women) were included as controls. The male-to-female ratio was not significantly different between the reticular pseudodrusen group and normal group (*P* = .648, x^2 test). The ages of the subjects ranged from 67–91 years (mean±SD, 79.4±6.6 years) for patients with reticular pseudodrusen and from 69-87 years (mean±SD, 77.1±5.4 years) for normal controls (*P* = .241, unpaired *t* test). The axial length ranged from 21.8-25.3 mm (mean± SD, 23.4±0.9 mm) in eyes with reticular pseudodrusen and 22.1-24.8 mm (mean±SD, 23.3±0.7 mm) in normal eyes (*P* = .582, unpaired *t* test). The mean visual acuity (logarithm of minimal angle of resolution; logMAR) was 0.24±0.38 in the reticular pseudodrusen group and -0.01±0.12 in the normal group, and eyes with reticular pseudodrusen had significantly poorer visual acuity (*P* < .001, Welch's *t* test) (Table 1).

The mean choroidal thickness and volume of each ETDRS sector was significantly reduced in eyes with reticular pseudodrusen compared with normal eyes (*P* < .020 for all, unpaired *t* test or Welch's *t* test) (Figures 2–4, Table 2). The central choroidal thickness and volume (1 mm diameter) in eyes with reticular pseudodrusen were 143.4 ±50.2 μm and 0.11±0.04 mm^3, respectively, which were significantly smaller than those in normal eyes (234.3±75.8 μm and 0.18±0.06 mm^3; *P* < .001, Welch's *t* test). Whole macular choroidal thickness and volume (6 mm diameter) in eyes with reticular pseudodrusen were 134.4±39.8 μm and 3.80±1.13 mm^3, respectively, which were significantly smaller than those in normal eyes (201.2±67.8 μm and 5.69±1.92 mm^3; *P* = .003, Welch's *t* test).

Eyes with reticular pseudodrusen were classified into 3 subgroups: eyes without late

AMD (Group 1, n = 20), eyes with neovascular AMD (Group 2, n = 10), and eyes with geographic atrophy (Group 3, n = 8). The mean age was 77.6±6.0, 81.8±7.9, and 81.1 ±5.9 years in Group 1, Group 2, and Group 3, respectively (*P* = .183, 1-way analysis of variance; Supplemental Table 1, available at AJO.com). The mean axial length was 23.2 ±0.9, 23.6±0.7, and 23.8±1.2mm in Group 1, Group 2, and Group 3, respectively. (*P* = .268, 1-way analysis of variance; Supplemental Table 1). The mean age and mean axial length of each subgroup were not statistically different compared with normal eyes (Table 3). The mean choroidal thickness and volume of each sector in the ETDRS showed no significant difference among Group 1, Group 2, and Group 3; however, most of them showed decreased thickness compared with normal eyes (Figures 1–4, Table 4, Supplemental Table 2, available at AJO.com). Central choroidal thickness and volume were 138.1±52.2 μm and 0.11±0.04 mm^3 in Group 1, 148.0±53.1 μm and 0.12±0.04 mm^3 in Group 2, and 151.2±45.9 μm and 0.12±0.04 mm^3 in Group 3, which were smaller than those of normal eyes (*P* < .001, *P* = .005, *P* =.011, respectively, unpaired *t* test). The mean whole macular choroidal thickness and volume was 129.3±40.6 μm and 3.66±1.15 mm^3 in Group 1, 135.8±46.3 μm and 3.84±1.31 mm^3 in Group 2, and 145.4±30.8 μm and 4.11±0.87 mm^3 in Group 3, which were smaller than that of normal eyes (*P* = .002, Welch's *t* test, *P* = .015, unpaired *t* test, *P* = .016, Welch's *t* test, respectively).

Group 1 eyes (without late AMD) were grouped into 2 subgroups according to whether reticular pseudodrusen covered more than half of the area or not in each ETDRS sector. Mean choroidal thickness did not differ between 2 subgroups in every sector (*P* > .100 for all; Supplemental Table 3, available at AJO.com). Areas with reticular pseudodrusen in the macula (6 mm diameter) did not correlate with whole macular choroidal thickness (*P* = .673).

In eyes with reticular pseudodrusen, the correlation between whole choroidal volume and axial length was marginal (R^2 = 0.100, *P* = .055). Whole macular choroidal volume did not correlate with age (*P* = .649) and visual acuity (*P* = .572).

En face images through the choroid revealed narrow and sparse choroidal vessels in eyes with reticular pseudodrusen (Figure 5). The area of choroidal vasculature (40.8% ±5.5%) was significantly reduced in eyes with reticular pseudodrusen but without geographic atrophy or CNV compared with that of normal eyes (45.3%±6.4%, *P* = .037, unpaired *t* test).

DISCUSSION

With the development of imaging techniques, it has been possible to examine the

details of choroidal structures; such examination has revealed that the choroid plays an important role in the pathogenesis of various diseases.[22–25,30,31] Although the pathophysiology of reticular pseudodrusen remains unknown, there is sufficient evidence to show that the underlying mechanism may involve choroidal vascular abnormalities, such as impaired choroidal filling as detected by IA.[14] Recently, using the EDI-OCT technique, several researchers reported that the choroidal thickness is decreased in eyes with reticular pseudodrusen.[17,26] Querques and associates[17] reported that, at most measurement points, the choroidal thickness of eyes with reticular pseudodrusen was thinner than that of eyes with early AMD. Switzer and associates[26] reported that among patients with early AMD, those with reticular pseudodrusen had a thinner choroid in the subfovea as compared with those without reticular pseudodrusen. However, in studies using EDI-OCT, choroidal thickness was indicated by representative values obtained at several points, such as the foveal center and at 500- to 1500-µm increments from the foveal center. These measurements tend to be influenced by focal thickening or thinning of the choroid or, more often, by irregularity of the chorioscleral border, as seen on OCT images.

Previous studies using the raster scan protocol of this prototype SS-OCT demonstrated that high-speed scanning coupled with high sensitivity can be used to obtain highly reproducible measurements of the choroidal thickness in both normal eyes and eyes with macular diseases.[28,32–35] In the current study, using 3D raster scanning images obtained by high-penetration SS-OCT, eyes with reticular pseudodrusen were found to have thinned and reduced-volume choroids in the whole macular area. In addition, the current study showed that although the mean choroidal thickness and volume of each area was not significantly different between eyes with CNV or geographic atrophy and those without both these conditions, eyes of all the patients with reticular pseudodrusen had decreased choroidal thickness and volume compared with normal eyes. These results suggest that macular choroidal thinning and reduced volume are related to reticular pseudodrusen itself, regardless of the occurrence of CNV or geographic atrophy.

To date, several investigators have reported that foveal choroidal thickness is correlated with age, axial length, or refractive error in normal subjects.[20,36] These results suggest that both age and axial length should be matched when comparing choroidal thickness. In the current study, age-matched normal controls were used, and the mean axial length of patients and normal controls was similar. We also found that the mean macular choroidal thickness and volume was marginally correlated with axial length in eyes with reticular pseudodrusen, suggesting that axial length should be taken into

consideration even when comparing pseudodrusen eyes. In the current study, no significant differences in axial length were noted among the subgroups of reticular pseudodrusen.

The origin of reticular pseudodrusen is still unknown. Arnold and associates[2] histopathologically examined 1 eye with the antemortem diagnosis of reticular pseudodrusen and estimated the reticular pattern in the deep layer of choroid. Later, the same group performed another histologic examination of an eye with reticular pseudodrusen, and reported debris in the subretinal space.[4] Zweifel and associates[37] studied eyes with reticular pseudodrusen using SD-OCT and indicated the possibility that reticular pseudodrusen were subretinal drusenoid deposits observed on histologic examination. A recent study by Curcio and associates[38] reported the histological findings in 22 donor eyes with AMD, which suggested that subretinal drusenoid deposits corresponded to reticular pseudodrusen. The findings were also supported by those of Schmitz-Valckenberg and associates[39] who used combined confocal scanning-laser ophthalmoscopy and SD-OCT to study eyes with reticular pseudodursen. On the other hand, several investigators have reported findings that support the idea that reticular pseudodrusen may represent choroidal changes. Sohrab and associates[18] reported that correlation of registered IR, FAF, and red-free images localized the reticular pattern to the intravascular choroidal stroma on en face OCT sections. Querques and associates[17] showed that the reticular patterns appeared as hypofluorescent lesions on IA, closely abutting but not overlying the large choroidal vessels. Thus, although further investigations are necessary to determine the exact origin of reticular pseudodrusen, choroidal involvement should be taken into consideration to its pathogenesis. Several studies have reported the abnormalities in the choroidal vascular structure in eyes with reticular pseudodrusen. A histologic report showed that small choroidal blood vessels were almost absent and larger vessels were also decreased in an eye with reticular pseudodrusen.[2] Another histologic report showed patchy loss of choroidal capillaries and a thin choroid in a pathologic specimen of reticular pseudodrusen.[4] In the current study, en face high-penetration SS-OCT images revealed that the choroidal vascular area of the Haller layer was decreased in eyes with reticular pseudodrusen but without CNV or geographic atrophy, compared with normal eyes. Taken together, our in vivo findings and previous histopathology data suggest that there may be a diffuse loss of small and large choroidal vessels, including choroidal capillaries, in eyes with reticular pseudodrusen, leading to choroidal thinning and reduced volume in the whole macular area prior to the development of CNV or geographic atrophy. Although choroidal thinning or reduced choroidal volume does not necessarily imply choroidal ischemia, these results

suggest that atrophy of the whole choroid may be involved in the occurrence or development of reticular pseudodrusen. The reduction of ischemic factors, such as reducing cholesterol/triglyceride levels, controlling blood pressure, and taking anticoagulant agents, may be a therapeutic strategy for slowing choroidal atrophy and ultimately reducing the risk for late AMD in patients with reticular pseudodrusen. Further studies are necessary to evaluate the relationship between the progression to late AMD, systemic diseases, and reticular pseudodrusen.

There are several limitations of this study. Although high-penetration SS-OCT increases the sensitivity of the choroid, light is still scattered by the RPE and choroid, which makes visualization of the chorioscleral interface difficult in a few images. In the current study, in B-scans where it was difficult to identify the whole outer choroid, 7-15 points where the chorioscleral interface could be identified were chosen and connected to create a segmentation line. There was no automated segmentation software available for measuring choroidal thickness for the SS-OCT prototype system; thus, all segmentations were performed manually. However, we have previously shown good interobserver repeatability with this technique.[28] Because this was a cross-sectional study, we might have overlooked stage 4 reticular pseudodrusen (fading of the subretinalmaterial because of reabsorption and migration within the inner retinal layers).[40] Recently, using multimodal imaging, Spaide[41] demonstrated that eyes with regression of reticular pseudodrusen develop outer retinal atrophy and loss of the underlying choroidal thickness. Thus, further assessment is necessary to evaluate the choroidal changes in stage 4 of reticular pseudodrusen.

In conclusion, our study revealed that macular choroidal thickness and volume in eyes with reticular pseudodrusen were significantly decreased, regardless of CNV or geographic atrophy. Furthermore, en face SS-OCT images showed that the choroidal vascular area was decreased in eyes with reticular pseudodrusen. Although it remains unknown whether choroidal thinning and choroidal vascular changes are causes or consequences of reticular pseudodrusen, the findings of this study may help to elucidate its pathogenesis. In the future, we hope to perform longitudinal studies using SS-OCT to further elucidate the involvement of the choroid in the pathogenesis of reticular pseudodrusen.

ACKNOWLEDGEMENTS

Funding/Support: This research was supported in part by the Grant-in-Aid for Scientific Research (21791679) from the Japan Society for the Promotion of Science (JSPS) and Topcon.

Financial disclosures: Nagahisa Yoshimura: advisory board of Topcon.

Author contribution: Conception and design (U.N.A., S.O.) Analysis and interpretation (N.U.A, S.O.) Writing the article (N.U.A., S.O.) Critical revision of the article (S.O., N.Y.) Final approval of the article (U.N.A., S.O., A.A.E., A.Takahashi, A.O., H.T., K.Y., A.Tsujikawa, N.Y.) Data collection (U.N.A., A.A.E., A.Takahashi) Provision of materials (S.O., A.O., H.T., K.Y., A.Tsujikawa., N.Y.) Statistical expertise (U.N.A., S.O.) Obtaining funding (S.O.) Literature search (N.U.A., S.O.)

References

1. Mimoun G, Soubrane G, Coscas G. Macular drusen. *J Fr Ophthalmol* 1990;13(10): 511-530.
2. Arnold JJ, Sarks SH, Killingsworth MC, Sarks JP. Reticular pseudodrusen. A risk factor in age-related maculopathy. *Retina* 1995;15(3):183-191.
3. Cohen SY, Dubois L, Tadayoni R, Delahaye-Mazza C, Debibie C, Quentel G. Prevalence of reticular pseudodrusen in age-related macular degeneration with newly diagnosed choroidal neovascularisation. *Br J Ophthalmol* 2007;91(3):354-359.
4. Sarks J, Arnold J, Ho IV, Sarks S, Killingsworth M. Evolution of reticular pseudodrusen. *Br J Ophthalmol* 2011;95(7):979-985.
5. Pumariega NM, Smith RT, Sohrab MA, Letien V, Souied EH. A prospective study of reticular macular disease. *Ophthalmology* 2011;118(8):1619-1625.
6. Schmitz-Valckenberg S, Alten F, Steinberg JS, et al. Reticular drusen associated with geographic atrophy in age-related macular degeneration. *Invest Ophthalmol Vis Sci* 2011;52(9):5009-5015.
7. Klein R, Meuer SM, Knudtson MD, Iyengar SK, Klein BE. The epidemiology of retinal reticular drusen. *Am J Ophthalmol* 2008;145(2):317-326.
8. Ueda-Arakawa N, Ooto S, Nakata I, et al. Prevalence and genomic association of reticular pseudodrusen in age-related macular degeneration. *Am J Ophthalmol* 2013; 155(2):260-269.e2.
9. Zweifel SA, Imamura Y, Spaide TC, Fujiwara T, Spaide RF. Prevalence and significance of subretinal drusenoid deposits (reticular pseudodrusen) in age-related macular degeneration. *Ophthalmology* 2010;117(9):1775-1781.
10. Lee MY, Yoon J, Ham DI. Clinical characteristics of reticular pseudodrusen in Korean patients. *Am J Ophthalmol* 2012;153(3):530-535.
11. Lee MY, Yoon J, Ham DI. Clinical features of reticular pseudodrusen according to the fundus distribution. *Br J Ophthalmol* 2012;96(9):1222-1226.
12. Querques G, Massamba N, Srour M, Boulanger E, Georges A, Souied EH. Impact of reticular pseudodrusen on macular function. *Retina*. In press.
13. Ooto S, Ellabban AA, Ueda-Arakawa N, et al. Reduction of retinal sensitivity in eyes with reticular pseudodrusen. *Am J Ophthalmol*. In press.
14. Smith RT, Sohrab MA, Busuoic M, Barile G. Reticular macular disease. *Am J Ophthalmol* 2009;148(5):733-743.e2.
15. Spaide RF, Curcio CA. Drusen characterization with multimodal imaging. *Retina* 2010;30(9):1441–1454.
16. Ueda-Arakawa N, Ooto S, Tsujikawa A, Yamashiro K, Oishi A, Yoshimura N.

Sensitivity and specificity of detecting reticular pseudodrusen in multimodal imaging in Japanese patients. *Retina* 2013;33(3):490-497.

17. Querques G, Querques L, Forte R, Massamba N, Coscas F, Souied EH. Choroidal changes associated with reticular pseudodrusen. *Invest Ophthalmol Vis Sci* 2012; 53(3):1258-1263.
18. Sohrab MA, Smith RT, Salehi-Had H, Sadda SR, Fawzi AA. Image registration and multimodal imaging of reticular pseudodrusen. *Invest Ophthalmol Vis Sci* 2011;52(8): 5743-5748.
19. Spaide RF, Koizumi H, Pozonni MC. Enhanced depth imaging spectral-domain optical coherence tomography. Am J Ophthalmol 2008;146(4):496-500.
20. Margolis R, Spaide RF. A pilot study of enhanced depth imaging optical coherence tomography of the choroid in normal eyes. *Am J Ophthalmol* 2009;147(5):811-5.
21. Imamura Y, Fujiwara T, Margolis R, Spaide RF. Enhanced depth imaging optical coherence tomography of the choroid in central serous chorioretinopathy. *Retina* 2009; 29(10):1469-1473.
22. Fujiwara T, Imamura Y, Margolis R, et al. Enhanced depth imaging optical coherence tomography of the choroid in highly myopic eyes. *Am J Ophthalmol* 2009;148(3):445-450.
23. Manjunath V, Goren J, Fujimoto JG, Duker JS. Analysis of choroidal thickness in age-related macular degeneration using spectral-domain optical coherence tomography. *Am J Ophthalmol* 2011;152(4):663-668.
24. Chung SE, Kang SW, Lee JH, Kim YT. Choroidal thickness in polypoidal choroidal vasculopathy and exudative age-related macular degeneration. *Ophthalmology* 2011; 118(5):840-845.
25. Jirarattanasopa P, Ooto S, Nakata I. Choroidal thickness, vascular hyperpermeability, and complement factor H in age-related macular degeneration and polypoidal choroidal vasculopathy. *Invest Ophthalmol Vis Sci* 2012;53(7):3663-3672.
26. Switzer DJ Jr, MendonÇa LS, Saito M, et al. Segregation of ophthalmoscopic characteristics according to choroidal thickness in patients with early age-related macular degeneration. *Retina*. 2012;32(7):1265-1271.
27. de Bruin DM, Burnes DL, Loewenstein J, et al. In vivo three-dimensional imaging of neovascular age-related macular degeneration using optical frequency domain imaging at 1050 nm. *Invest Ophthalmol Vis Sci* 2008;49(10):4545-4552.
28. Hirata M, Tsujikawa A, Matsumoto A, et al. Macular choroidal thickness and volume in normal subjects measured by swept-source optical coherence tomography. *Invest Ophthalmol Vis Sci* 2011;52(8):4971-4978.

29. Keane P, Ruiz-Garcia H, Sadda S. Clinical applications of long-wavelength (1,000-nm) optical coherence tomography. *Ophthalmic Surg Lasers Imaging* 2011;42(suppl): S67-74.
30. Jirarattanasopa P, Ooto S, Tsujikawa A, et al. Assessment of macular choroidal thickness by optical coherence tomography and angiographic changes in central serous chorioretinopathy. *Ophthalmology* 2012;119(8):1666-1678.
31. Spaide RF. Age-related choroidal atrophy. *Am J Ophthalmol* 2009;147(5):801-10.
32. Ellabban AA, Tsujikawa A, Matsumoto A, et al. Three-dimensional tomographic features of dome-shaped macula by swept-source optical coherence tomography. *Am J Ophthalmol* 2013;155(2):320-328.e2.
33. Ellabban A, Tsujikawa A, Matsumoto A, et al. Macular choroidal thickness and volume in eyes with angioid streaks measured by swept source optical coherence tomography. *Am J Ophthalmol* 2012;153(6):1133-1143.
34. Ellabban AA, Tsujikawa A, Matsumoto A, et al. Macular choroidal thickness measured by swept source optical coherence tomography in eyes with inferior posterior staphyloma. *Invest Ophthalmol Vis Sci* 2012;53(12):7735-7745.
35. Ellabban AA, Tsujikawa A, Ooto S, et al. Focal choroidal excavation in eyes with central serous chorioretinopathy. *Am J Ophthalmol* 2013;156(4):673-683.e1.
36. Ikuno Y, Kawaguchi K, Nouchi T, Yasuno Y. Choroidal thickness in healthy Japanese subjects. *Invest Ophthalmol Vis Sci* 2010;51(4):2173-2176.
37. Zweifel SA, Spaide RF, Curcio CA, Malek G, Imaura Y. Reticular pseudodrusen are subretinal drusenoid deposits. *Ophthalmology*. 2010;117(2):303-312.e1.
38. Curcio CA, Messinger JD, Sloan KR, McGwin G, Medeiros NE, Spaide RF. Subretinal drusenoid deposits in non-neovascular age-related macular degeneration: morphology, prevalence, topography, and biogenesis model. *Retina* 2013;33(2):265-276.
39. Schmitz-Valckenberg S, Steinberg JS, Fleckenstein M, Visvalingam S, Brinkmann CK, Holz FG. Combined confocal scanning laser ophthalmoscopy and spectral-domain optical coherence tomography imaging of reticular drusen associated with age-related macular degeneration. *Ophthalmology* 2010;117(6):1169-1176.
40. Querques G, Canouï-Poitrine F, Coscas F, et al. Analysis of progression of reticular pseudodrusen by spectral domain–optical coherence tomography. *Invest Ophthalmol Vis Sci* 2012;53(3):1264-1270.
41. Spaide RF. Outer retinal atrophy after regression of subretinal drusenoid deposits as newly recognized form of late age-related macular degeneration. *Retina* 2013;33(9): 1800-1808.

FIGURE 1. A choroidal thickness map obtained by high-penetration swept-source optical coherence tomography (SS-OCT) in a normal eye of a 74-year-old man. (Top left) Three-dimensional raster scan covering a 6×6 mm area centered on the fovea. The Early Treatment Diabetic Retinopathy Study (ETDRS) sectors were applied to the scanned area, and the mean choroidal thickness of 9 sectors was measured. (Top right) The ETDRS sectors consist of a “center” sector within 0.5 mm from the center of the fovea, 4 “inner ring” sectors (nasal, superior, temporal, and inferior) 0.5–1.5 mm from the center of the fovea, and 4 “outer ring” sectors (nasal, superior, temporal, and inferior) 1.5–3.0 mm from the center of the fovea. (Bottom left) B-scan images at different levels of the raster scan. (Bottom right) Green segmentation lines show Bruch membrane and the chorioscleral border.

FIGURE 2. Macular choroidal thickness in the left eye of an 82-year-old man with reticular pseudodrusen but without choroidal neovascularization or geographic atrophy (Group 1). (Top left) Color fundus photography shows numerous reticular pseudodrusen and some soft drusen. (Top middle) Infrared reflectance image shows reticular pseudodrusen lesions as a group of hyporeflectant lesions or target-like lesions against a background of mild hyper-reflectance (within dotted lines). (Top right) Fundus autofluorescence (FAF) shows reticular pseudodrusen lesions as a group of ill-defined, hypofluorescent lesions against a background of mildly elevated autofluorescence (within dotted lines). Horizontal (Second row) and vertical (Third row) SS-OCT (12mm scan) images thorough the fovea, in the direction of the green arrows in color fundus photography (at Top left), show reticular pseudodrusen lesions identified as hyperreflective mounds or triangular lesions above the retinal pigment epithelium, soft drusen, and thin choroid. (Bottom left) Choroidal thickness map of 6 × 6 mm of the macular area created from the 3-dimensional raster scan data set. (Bottom right) By applying the ETDRS grid to the map, mean choroidal thickness was obtained in each sector. Choroidal thickness was reduced in the whole macula.

FIGURE 3. Macular choroidal thickness in the right eye of an 82-year-old man with reticular pseudodrusen and choroidal neovascularization (Group 2). (Top left) Color fundus photography shows numerous reticular pseudodrusen (within dotted lines) and choroidal neovascularization. (Top middle) Infrared reflectance image shows reticular pseudodrusen lesions (within dotted lines). (Top right) Fluorescein angiography shows choroidal neovascularization. Horizontal (Second row) and vertical (Third row) SS-OCT (12 mm scan) images thorough the fovea, in the direction of the green arrows in color

fundus photography (at Top left), show reticular pseudodrusen lesions, serous retinal detachment, choroidal neovascularization, and thin choroid. (Bottom left and Bottom right) Choroidal thickness map shows reduced choroidal thickness in the whole macula.

FIGURE 4. Macular choroidal thickness in the eye of a 76-year-old woman with reticular pseudodrusen and geographic atrophy (Group 3). (Top left) Color fundus photography shows numerous reticular pseudodrusen and geographic atrophy. (Top middle) Infrared reflectance image shows reticular pseudodrusen lesions (within dotted lines). (Top left) FAF shows reticular pseudodrusen lesions (within dotted lines) and hypofluorescence corresponding to the area with geographic atrophy. Horizontal (Second row) and vertical (Third row) SS-OCT (12 mm scan) images thorough the fovea, in the direction of the green arrows in color fundus photography (top left), show reticular pseudodrusen lesions, increased light penetration to the choroid in the area with geographic atrophy, and thin choroid. (Bottom left and Bottom right) Choroidal thickness map shows reduced choroidal thickness in the whole macula.

FIGURE 5. En face images of the choroidal vasculature in a normal eye (Top left, middle and right) and an eye with reticular pseudodrusen (Bottom left, middle and right). En face images were reconstructed from a 3-dimensional raster scan data set by flattening the images at the Bruch membrane level. The middle layer between Bruch membrane and the deepest level of the chorioscleral border (Top left and Bottom left) shows the structures of choroidal vasculature (Top middle and Bottom middle). Then Image J software was used to automatically detect the choroidal vascular area (Top right and Bottom right). Note that the area with choroidal vessels is decreased in an eye with reticular pseudodrusen compared with a normal eye.

TABLE 1. Characteristics of Eyes With Reticular Pseudodrusen and Those of Normal Controls in This Study

	Eyes with reticular pseudodrusen (n = 38)	Normal controls (n = 14)	*P*
Male-to-female ratio	19/19	6/8	0.648*
Mean age (y)	79.4 ± 6.6	77.1 ± 5.4	0.241**
Mean axial length (mm)	23.4 ± 0.9	23.3 ± 0.7	0.582**
Visual acuity (logMAR)	0.24 ± 0.38	-0.01 ± 0.12	< 0.001***

logMAR = logarithm of minimal angle resolution.

All values are presented as mean ± standard deviation.

* χ^2 test.

**Unpaired *t* test.

***Welch's *t* test.

TABLE 2. Comparison of Choroidal Thickness and Volume Between Eyes With Reticular Pseudodursen and Normal Eyes

	Mean choroidal thickness (μm)		Mean choroidal volume (mm^3)		*P*
Area	Eyes with reticular pseudodrusen (n = 38)	Normal eyes (n = 14)	Eyes with reticular pseudodrusen (n = 38)	Normal eyes (n = 14)	
Center	143.4 ± 50.2	234.3 ± 75.8	0.11 ± 0.04	0.18 ± 0.06	< 0.001*
Inner temporal	150.4 ± 47.1	228.6 ± 70.5	0.24 ± 0.07	0.36 ± 0.11	< 0.001**
Inner superior	144.0 ± 48.2	230.7 ± 79.7	0.23 ± 0.08	0.36 ± 0.13	0.001*
Inner nasal	127.5 ± 47.1	211.8 ± 74.5	0.20 ± 0.07	0.33 ± 0.12	0.001*
Inner inferior	136.2 ± 51.1	211.2 ± 72.2	0.21 ± 0.08	0.33 ± 0.11	< 0.001**
Outer temporal	145.7 ± 40.0	197.8 ± 65.2	0.77 ± 0.21	1.05 ± 0.35	0.012*
Outer superior	142.3 ± 42.9	223.0 ± 77.5	0.75 ± 0.23	1.18 ± 0.41	0.002*
Outer nasal	106.2 ± 35.6	168.1 ± 70.5	0.56 ± 0.19	0.89 ± 0.37	0.007*
Outer inferior	136.2 ± 43.6	188.0 ± 67.1	0.72 ± 0.23	1.00 ± 0.36	0.016*
Whole macula	134.4 ± 39.8	201.2 ± 67.8	3.80 ± 1.13	5.69 ± 1.92	0.003*

All values are presented as the mean ± standard deviation

Center = within 0.5 mm from the foveal center; Inner = 0.5–1.5 mm from the foveal center; Outer = 1.5–3.0 mm from the foveal center; Whole = within 3.0 mm from the foveal center.

*Welch's *t* test

**Unpaired *t* test

TABLE 3. Comparison of Mean Age and Axial Length Between Eyes With Reticular Pseudodrusen and Normal Eyes

	Group 1 (n = 20)	Group 2 (n = 10)	Group 3 (n = 8)	Normal (n = 14)	*P**	*P***	*P****
Mean age	77.6 ± 6.0	81.8 ± 7.9	81.1 ± 5.9	77.1 ± 5.4	0.813	0.094	0.117
Mean axial length (mm)	23.2 ± 0.9	23.6 ± 0.7	23.8 ± 1.2	23.3 ± 0.7	0.790	0.290	0.227

All values are presented as the mean ± standard deviation

Group 1: eyes with reticular pseudodrusen and without late age-related macular degeneration (AMD)

Group 2: eyes with reticular pseudodrusen and exudative AMD,

Group 3: eyes with reticular pseudodrusen and geographic atrophy.

*Comparison between Group 1 and normal eyes by unpaired *t* test or Welch's *t* test.

**Comparison between Group 2 and normal eyes by unpaired *t* test or Welch's *t* test.

***Comparison between Group 3 and normal eyes by unpaired *t* test or Welch's *t* test.

TABLE 4. Comparison of Mean Choroidal Thickness and Volume of Eyes With Reticular Pseudodrusen in Each Subgroup With Normal Eyes

	Mean choroidal thickness (μm)				Mean choroidal volume (mm^3)				*P**	*P***	*P****
Area	Group 1 (n = 20)	Group 2 (n = 10)	Group 3 (n = 8)	Normal (n = 14)	Group 1 (n = 20)	Group 2 (n = 10)	Group 3 (n = 8)	Normal (n = 14)			
Center	138.1 ± 52.2	148.0 ± 53.1	151.2 ± 45.9	234.3 ± 75.8	0.11 ± 0.04	0.12 ± 0.04	0.12 ± 0.04	0.18 ± 0.06	< 0.001	0.005	0.011
Inner temporal	145.9 ± 49.7	149.6 ± 47.1	162.6 ± 44.0	228.6 ± 0.5	0.23 ± 0.08	0.23 ± 0.07	0.26 ± 0.07	0.36 ± 0.11	< 0.001	0.006	0.027
Inner superior	138.8 ± 54.3	145.5 ± 46.4	155.0 ± 36.1	230.7 ± 79.7	0.22 ± 0.09	0.23 ± 0.07	0.24 ± 0.06	0.36 ± 0.13	< 0.001	0.006	0.007
Inner nasal	121.2 ± 49.2	130.9 ± 53.4	139.0 ± 34.5	211.8 ± 74.5	0.19 ± 0.08	0.21 ± 0.08	0.22 ± 0.05	0.33 ± 0.12	< 0.001	0.008	0.006
Inner inferior	129.2 ± 49.0	141.0 ± 61.7	147.7 ± 45.3	211.2 ± 72.2	0.20 ± 0.08	0.22 ± 0.10	0.23 ± 0.07	0.33 ± 0.11	< 0.001	0.021	0.037
Outer temporal	140.7 ± 39.2	144.9 ± 43.9	159.2 ± 38.4	197.8 ± 65.2	0.75 ± 0.21	0.77 ± 0.23	0.84 ± 0.20	1.05 ± 0.35	0.008	0.037	0.143
Outer superior	139.2 ± 44.8	139.6 ± 46.6	153.4 ± 35.9	223.0 ± 77.5	0.74 ± 0.24	0.74 ± 0.25	0.81 ± 0.19	1.18 ± 0.41	0.002	0.006	0.010
Outer nasal	101.0 ± 36.6	107.5 ± 42.4	117.7 ± 22.9	168.1 ± 70.5	0.53 ± 0.19	0.57 ± 0.22	0.62 ± 0.12	0.89 ± 0.37	0.004	0.025	0.025
Outer inferior	130.4 ± 38.6	141.8 ± 62.4	143.6 ± 28.1	188.0 ± 67.1	0.69 ± 0.20	0.75 ± 0.33	0.76 ± 0.15	1.00 ± 0.36	0.009	0.102	0.044
Whole macula	129.3 ± 40.6	135.8 ± 46.3	145.4 ± 30.8	201.2 ± 67.8	3.66 ± 1.15	3.84 ± 1.31	4.11 ± 0.87	5.69 ± 1.92	0.002	0.015	0.016

All values are presented as the mean ± standard deviation

Center = within 0.5 mm from the foveal center; Inner = 0.5–1.5mm from the foveal center; Outer = 1.5–3.0mm from the foveal center;

Whole = within 3.0 mm from the foveal center.

Group 1: eyes with reticular pseudodrusen and without late age-related macular degeneration (AMD)

Group 2: eyes with reticular pseudodrusen and exudative AMD,

Group 3: eyes with reticular pseudodrusen and geographic atrophy.

*Comparison between Group 1 and normal eyes by the unpaired *t* test or Welch's *t* test

**Comparison between Group 2 and normal eyes by the unpaired *t* test or Welch's *t* test

***Comparison between Group 3 and normal eyes by the unpaired *t* test or Welch's *t* test

SUPPLEMENTARY TABLE 1. Comparison of Mean Age and Axial Length of Eyes With Reticular Pseudodrusen Among 3 Subgroups.

	Group 1 (n = 20)	Group 2 (n = 10)	Group 3 (n = 8)	*P**	*P***	*P****	*P*****
Mean age	77.6 ± 6.0	81.8 ± 7.9	81.1 ± 5.9	0.183	0.218	0.389	0.973
Mean axial length (mm)	23.2 ± 0.9	23.6 ± 0.7	23.8 ± 1.2	0.268	0.503	0.296	0.910

All values are presented as the mean ± standard deviation

Group 1: eyes with reticular pseudodrusen and without late age-related macular degeneration (AMD)

Group 2: eyes with reticular pseudodrusen and exudative AMD,

Group 3: eyes with reticular pseudodrusen and geographic atrophy

*Comparison between the 3 subgroups by 1-way analysis of variance

**Comparison between Group 1 and Group 2 by the Tukey–Kramer test

***Comparison between Group 1 and Group 3 by the Tukey–Kramer test

****Comparison between Group 2 and Group 3 by the Tukey–Kramer test

SUPPLEMENTARY TABLE 2. Comparison of Mean Choroidal Thickness and Volume of Eyes With Reticular Pseudodrusen Among 3 Subgroups.

	Mean choroidal thickness (μm)			Mean choroidal volume (mm^3)			*P**	*P***	*P****	*P*****
Area	Group 1 (n = 20)	Group 2 (n = 10)	Group 3 (n = 8)	Group 1 (n = 20)	Group 2 (n = 10)	Group 3 (n = 8)				
Center	138.1 ± 52.2	148.0 ± 53.1	151.2 ± 45.9	0.11 ± 0.04	0.12 ± 0.04	0.12 ± 0.04	0.787	0.871	0.811	0.990
Inner temporal	145.9 ± 49.7	149.6 ± 47.1	162.6 ± 44.0	0.23 ± 0.08	0.23 ± 0.07	0.26 ± 0.07	0.708	0.979	0.681	0.832
Inner superior	138.8 ± 54.3	145.5 ± 46.4	155.0 ± 36.1	0.22 ± 0.09	0.23 ± 0.07	0.24 ± 0.06	0.731	0.934	0.708	0.910
Inner nasal	121.2 ± 49.2	130.9 ± 53.4	139.0 ± 34.5	0.19 ± 0.08	0.21 ± 0.08	0.22 ± 0.05	0.654	0.857	0.646	0.932
Inner inferior	129.2 ± 49.0	141.0 ± 61.7	147.7 ± 45.3	0.20 ± 0.08	0.22 ± 0.10	0.23 ± 0.07	0.662	0.827	0.671	0.959
Outer temporal	140.7 ± 39.2	144.9 ± 43.9	159.2 ± 38.4	0.75 ± 0.21	0.77 ± 0.23	0.84 ± 0.20	0.552	0.960	0.516	0.733
Outer superior	139.2 ± 44.8	139.6 ± 46.6	153.4 ± 35.9	0.74 ± 0.24	0.74 ± 0.25	0.81 ± 0.19	0.721	1.000	0.713	0.781
Outer nasal	101.0 ± 36.6	107.5 ± 42.4	117.7 ± 22.9	0.53 ± 0.19	0.57 ± 0.22	0.62 ± 0.12	0.539	0.883	0.507	0.820
Outer inferior	130.4 ± 38.6	141.8 ± 62.4	143.6 ± 28.1	0.69 ± 0.20	0.75 ± 0.33	0.76 ± 0.15	0.700	0.781	0.753	0.996
Whole macula	129.3 ± 40.6	135.8 ± 46.3	145.4 ± 30.8	3.66 ± 1.15	3.84 ± 1.31	4.11 ± 0.87	0.635	0.910	0.607	0.868

All values are presented as the mean ± standard deviation

Center = within 0.5 mm from the foveal center; Inner = 0.5–1.5mm from the foveal center; Outer = 1.5–3.0mm from the foveal center;

Whole = within 3.0 mm from the foveal center

Group 1: eyes with reticular pseudodrusen and without late age-related macular degeneration (AMD)

Group 2: eyes with reticular pseudodrusen and exudative AMD,

Group 3: eyes with reticular pseudodrusen and geographic atrophy

*Comparison between the 3 subgroups by 1-way analysis of variance

**Comparison between Group 1 and Group 2 by the Tukey–Kramer test

***Comparison between Group 1 and Group 3 by the Tukey–Kramer test

****Comparison between Group 2 and Group 3 by the Tukey–Kramer test

SUPPLEMENTARY TABLE 3. Comparison of Mean Choroidal Thickness in Each ETDRS Sector; 20 Eyes With Reticular Pseudodrusen Without Late AMD (Group 1) were Grouped into 2 Subgroups According to Whether Reticular Pseudodrusen Covered More or Less Than Half of Each Area

Area	Reticular pseudodrusen covered more than half of the area		Reticular pseudodrusen covered less than half of the area		*P**
	Mean choroidal thickness (μm)	Number of eyes	Mean choroidal thickness (μm)	Number of eyes	
Center	125.1 ± 26.5	8	146.7 ± 63.8	12	0.700
Inner temporal	141.1 ± 31.6	16	165.5 ± 100.2	4	0.925
Inner superior	140.7 ± 57.0	18	122.0 ± 8.8	2	0.529
Inner nasal	131.6 ± 55.9	13	101.9 ± 27.5	7	0.322
Inner inferior	129.5 ± 34.2	13	128.7 ± 72.5	7	0.191
Outer temporal	141.6 ± 20.5	13	138.9 ± 63.4	7	0.122
Outer superior	141.6 ± 44.7	19	93.6	1	N/A
Outer nasal	103.0 ± 41.5	12	97.9 ± 30.2	8	0.758
Outer inferior	130.4 ± 28.2	9	130.4 ± 46.9	11	0.621

All values are presented as the mean ± standard deviation

Center = within 0.5 mm from the foveal center; Inner = 0.5–1.5 mm from the foveal center; Outer = 1.5–3.0 mm from the foveal center

Whole = within 3.0 mm from the foveal center

*Mann–Whitney *U* test

FIGURE 1.

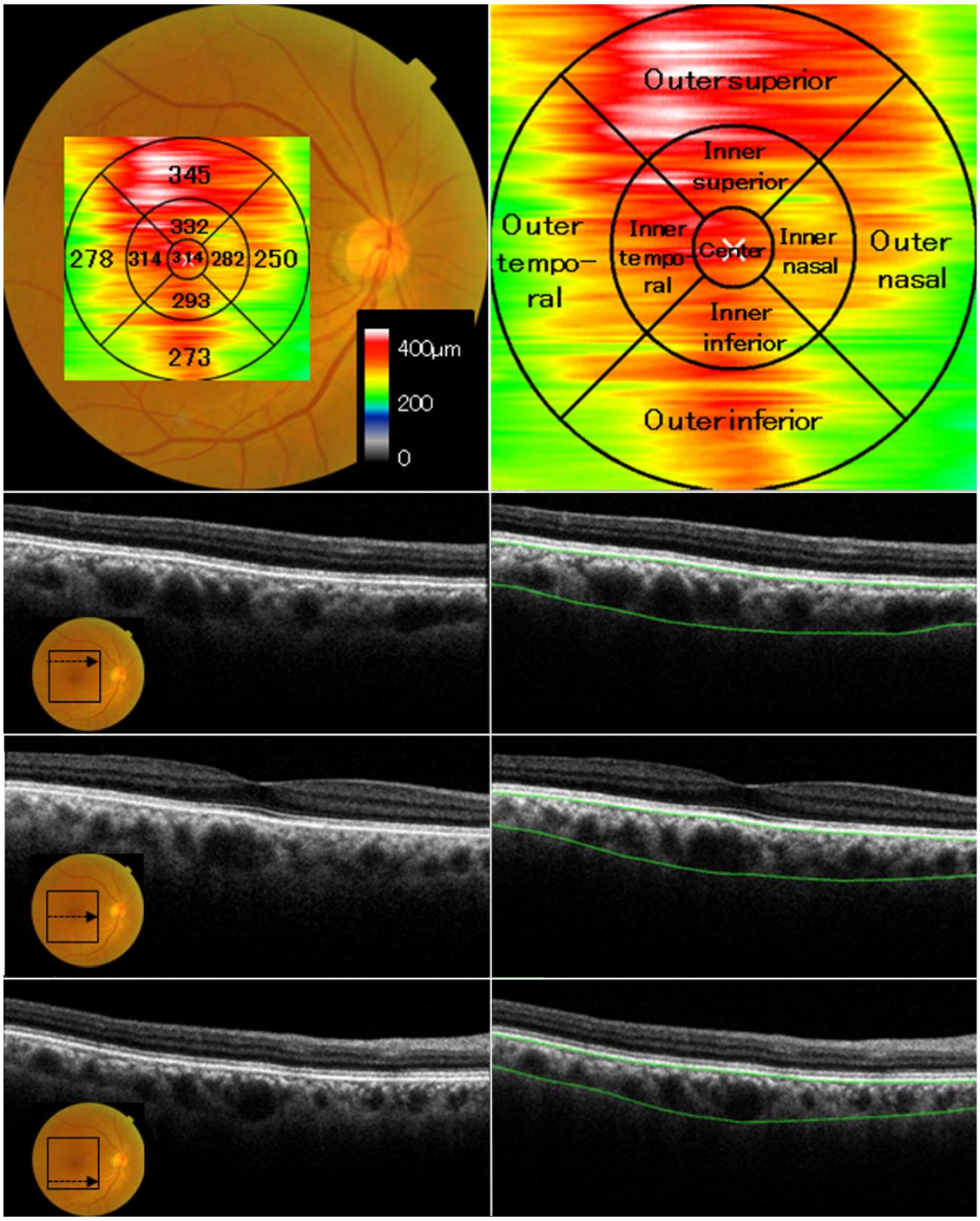
345
332
278
314
314
282
250
293
273
400μm
200
0
Outer superior
Inner superior
Outer temporal
Inner temporal
Center
Inner nasal
Outer nasal
Inner inferior
Outer inferior

FIGURE 2.

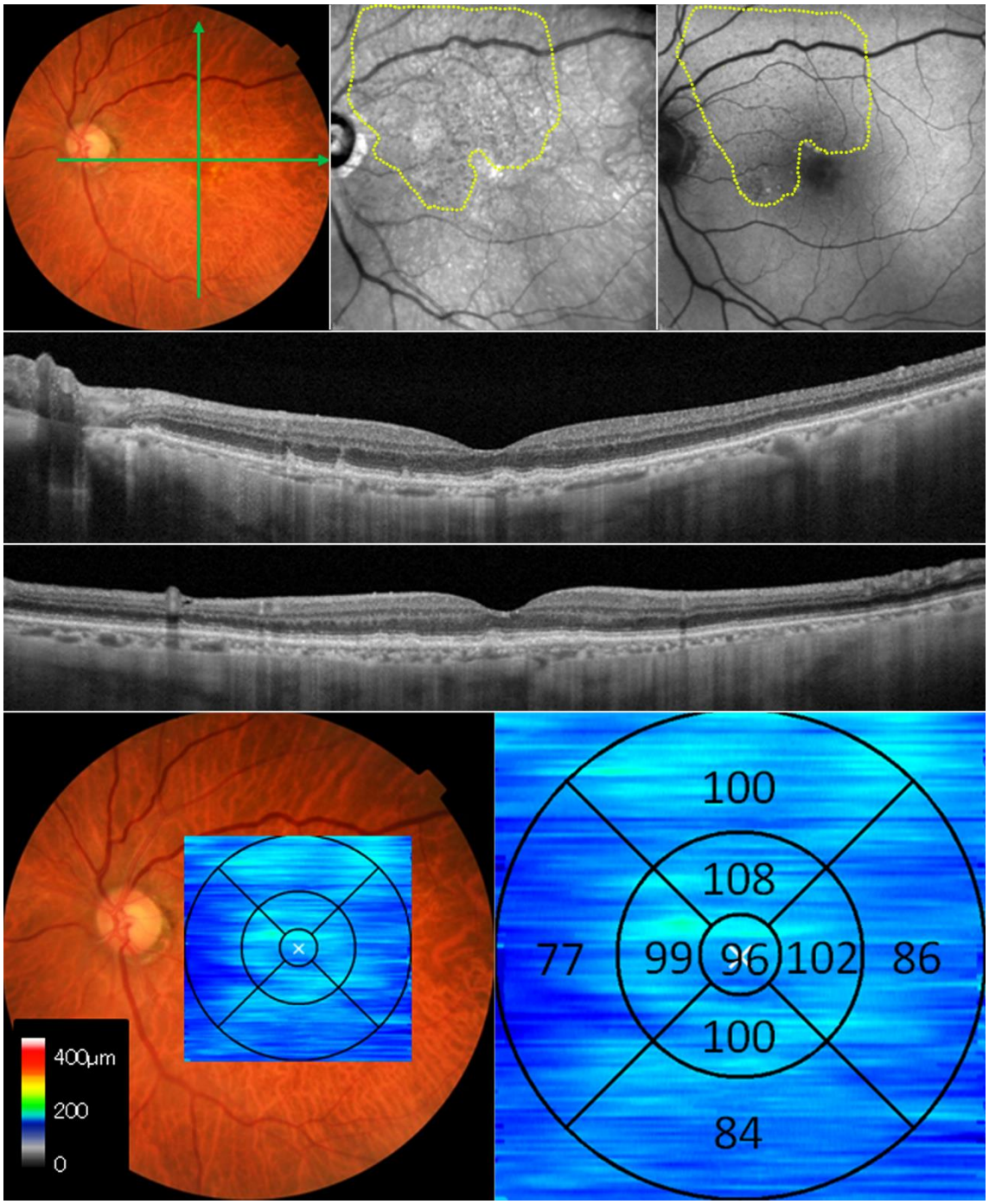

FIGURE 3.

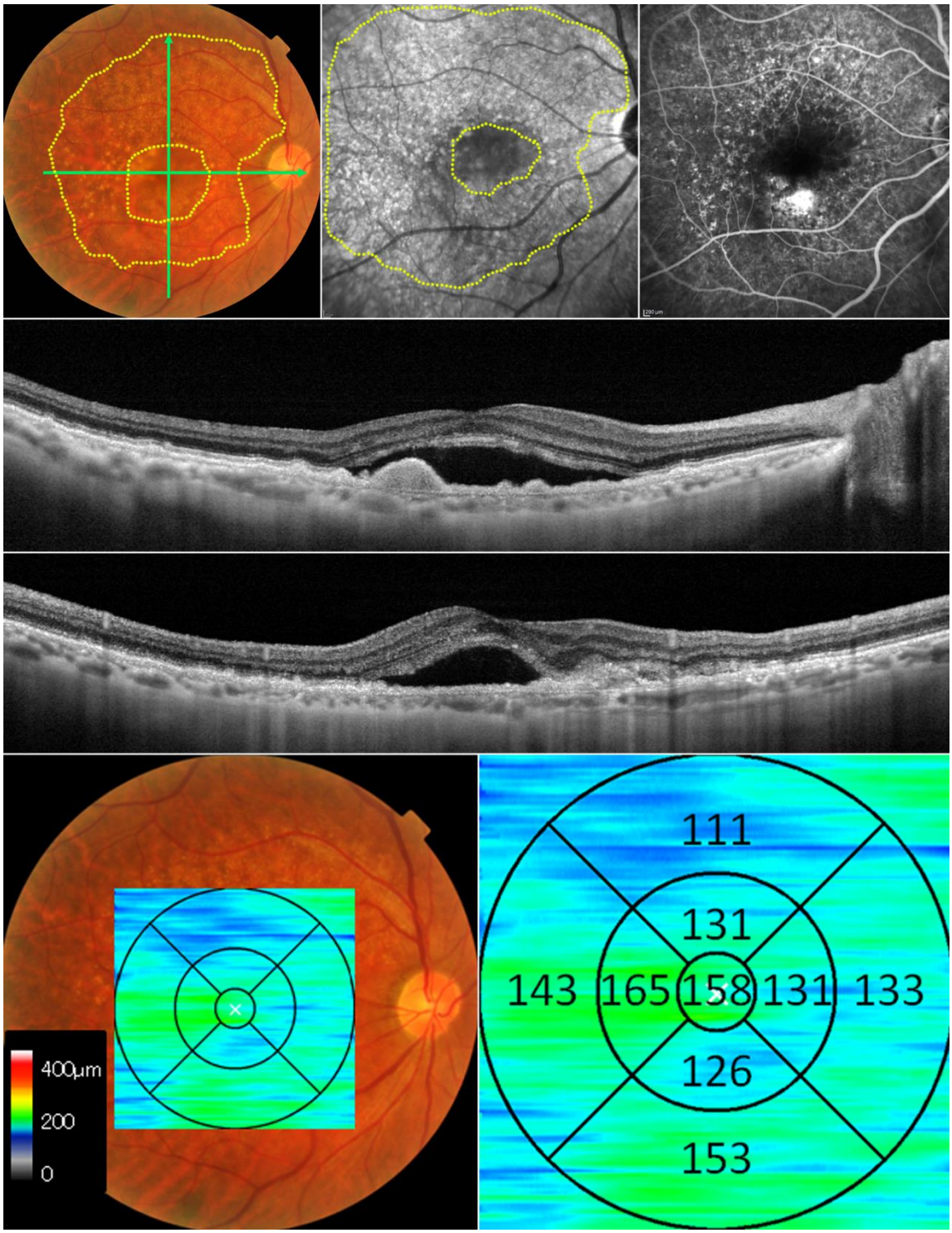

FIGURE 4.

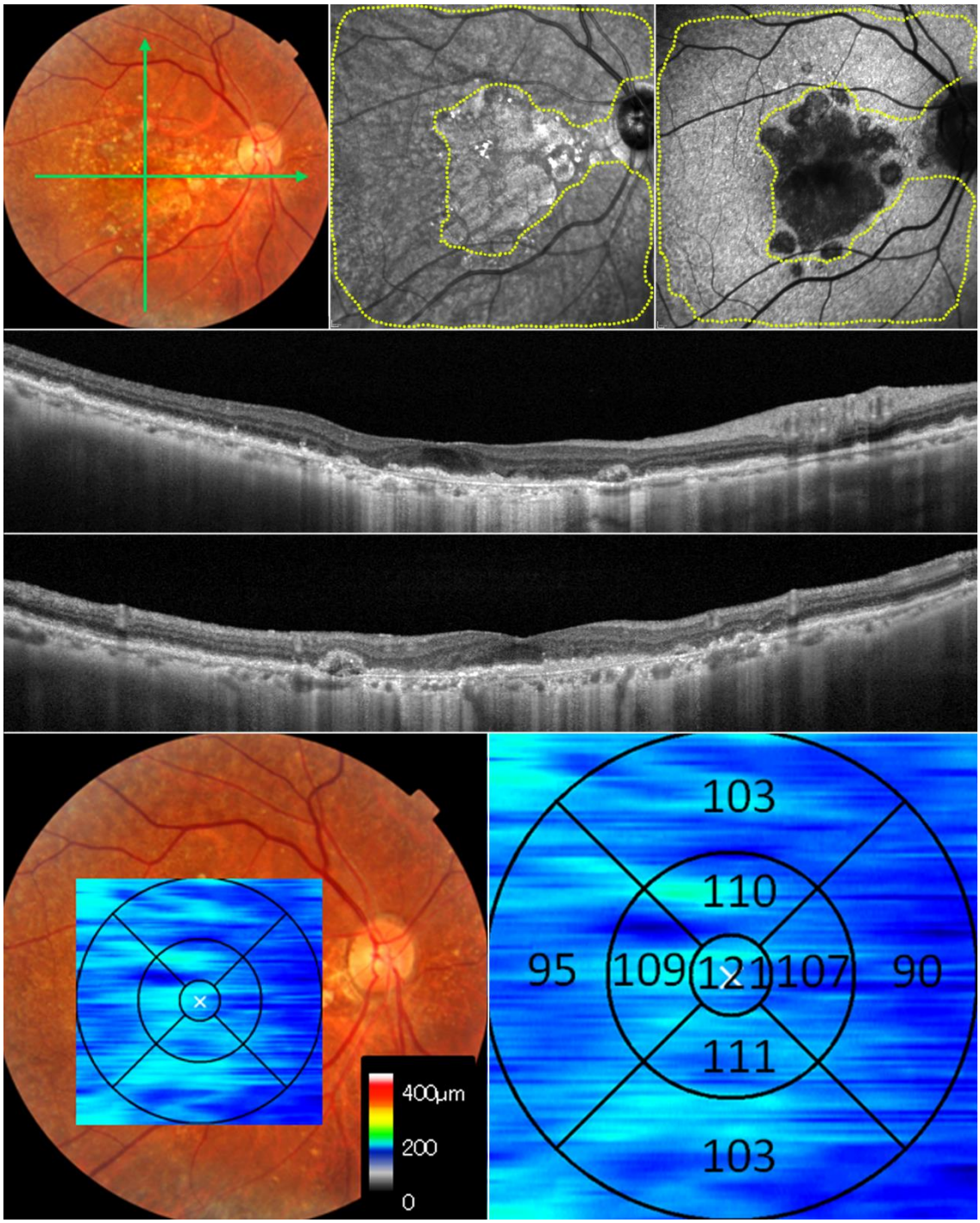
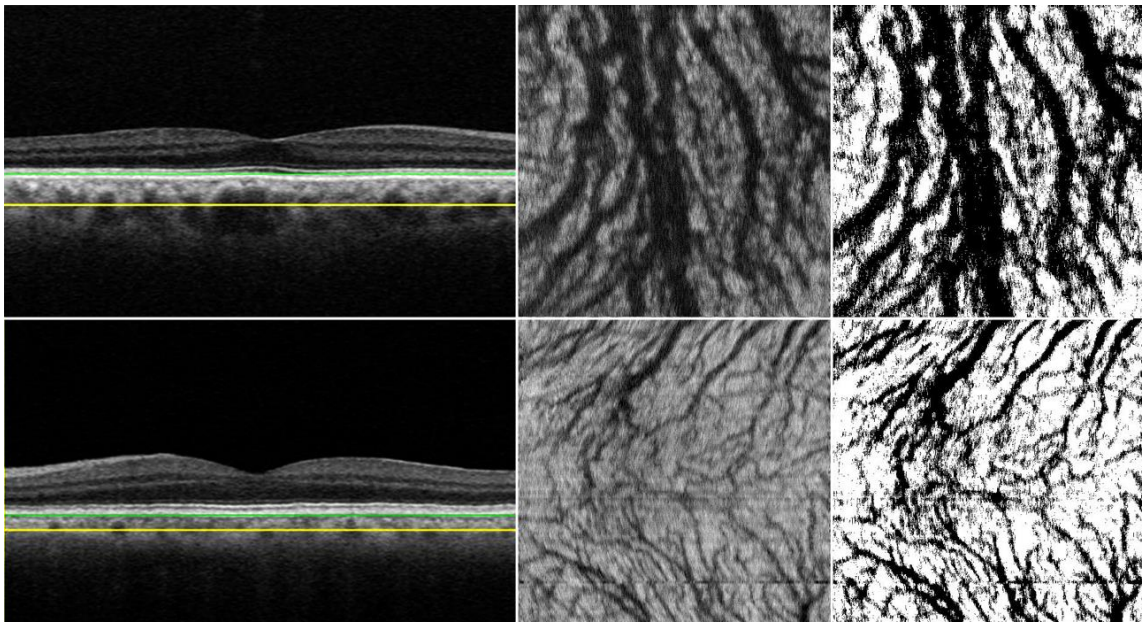
FIGURE 5.